

Tetrahedrite stability relations in the Cu-Fe-Sb-S system

KIYOAKI TATSUKA¹ AND NOBUO MORIMOTO

*Institute of Scientific and Industrial Research
Osaka University, Suita 565, Japan*

Abstract

Tetrahedrite forms a stable cone-shape solid solution at 500°C in the quaternary Cu-Fe-Sb-S composition tetrahedron, extending from its base with a narrow composition field on the Cu-Sb-S face to the top of composition $\text{Cu}_{10}\text{Fe}_2\text{Sb}_4\text{S}_{13}$. With the composition change from $\text{Cu}_{12.3}\text{Sb}_4\text{S}_{13}$ to $\text{Cu}_{10}\text{Fe}_2\text{Sb}_4\text{S}_{13}$ in the solid solution, the cell edge, melting temperature, and Vickers micro-hardness increase regularly from 10.3260 to 10.3835 Å, from 573° to 661°C, and from 300 to 380 kg/mm², respectively, whereas the density decreases from 5.00 to 4.81. Although iron-free tetrahedrite $\text{Cu}_{12}\text{Sb}_4\text{S}_{13}$ decomposes below 250°C, iron-bearing tetrahedrite such as $\text{Cu}_{11.5}\text{Fe}_{0.5}\text{Sb}_4\text{S}_{13}$ persists till room temperature.

Tetrahedrite solid solution is the only stable quaternary phase inside the Cu-Fe-Sb-S system and coexists with all the binary and ternary sulfide phases of the Cu-Fe-Sb-S system at 500°C, except covellite.

Introduction

Tetrahedrite contains many elements such as Fe, Zn, Ag, Hg, and/or As in addition to the three essential elements of Cu, Sb and S. This suggests that these guest elements may play important roles for the stability of tetrahedrite. In order to elucidate the stability relations of tetrahedrite in general, a study of the phase relations in quaternary systems such as the Cu-Fe-Sb-S and Cu-Zn-Sb-S is necessary.

The phases and phase relations in the Cu-Sb-S system have been reported by Skinner *et al.* (1972). Subsequently, the composition variations and phase relations of tetrahedrite and pseudotetrahedrite in the Cu-Sb-S system have been reported by Tatsuka and Morimoto (1973, 1977). Substitution of Cu by Zn, Fe, and Ag in synthetic tetrahedrite was studied by Hall (1972, 1974). Differential thermal analysis of synthetic tetrahedrite with iron was reported by Sugaki *et al.* (1972), and phase relations in the Cu-Fe-Sb-S system at 475°C, especially in the vicinities of the tetrahedrite solid solution and bornite solid solution, were reported by Nakamura *et al.* (1974).

In the Cu-Sb-S system (Tatsuka and Morimoto, 1973, 1977), the tetrahedrite solid solution at 500°C

does not contain the ideal composition, $\text{Cu}_{12}\text{Sb}_4\text{S}_{13}$, but occupies a narrow, more copper-rich composition field from $\text{Cu}_{12.28}\text{Sb}_{4.07}\text{S}_{13}$ to $\text{Cu}_{13.02}\text{Sb}_{4.01}\text{S}_{13}$. Tetrahedrite in this solid-solution field decomposes into famatinite, digenite, and antimony on annealing at temperatures below 250°C. However, tetrahedrite persists without this decomposition by rapid cooling to above 95°C; it dissociates into immiscible Cu-rich and Cu-poor metastable tetrahedrite phases by rapid cooling to below 95°C.

In some preliminary experiments, however, we observed that such decomposition and dissociation reactions did not occur when a small amount of iron replaced copper of tetrahedrite in the Cu-Sb-S ternary system (Tatsuka and Morimoto, 1973, 1977). This indicates that the stability region of tetrahedrite is essentially dependent on the amount of iron in the Cu-Fe-Sb-S system. In the present investigation, the phase relations and the stability regions of tetrahedrite in the Cu-Fe-Sb-S system have been determined, mainly from synthetic experiments at about 500°C. Additional experiments have been carried out at lower temperatures. The name abbreviations used in this study are given in Figure 1 and Table 1.

Experimental procedures

Elements of high purity were used as starting materials. Copper grains and iron sponge of 99.99 percent

¹ Present address: Osaka Custom House, Minato-ku, Osaka 552, Japan.

Table I. Composition and name abbreviation of natural and synthetic phases in the Cu-Fe-Sb-S system

System	Name	Abbreviation	Composition
Cu-S	covellite	cv	CuS
	chalcocite	cc	Cu ₂ S
	high digenite	hdg	Cu ₂ S - Cu _{1.75} S
Fe-S	pyrrhotite solid solution	po ss	Fe _{1-x} S
	pyrite	py	Fe ₂ S
Cu-Sb-S	famatinite	fm	Cu ₃ SbS ₄
	chalcostibite	cstb	CuSbS ₂
	tetrahedrite solid solution	td ss	Cu _{12+x} Sb _{4+y} S ₁₃
	pseudotetrahedrite solid solution	ptd ss	Cu ₃ SbS ₃ — Cu _{12.39} Sb _{4.54} S ₁₃
	skinnerite	sk	Cu ₃ SbS ₃
Cu-Fe-S	bornite	bn	Cu ₅ FeS ₄
	bornite solid solution	bn ss	wide range
	chalcopyrite	cp	CuFeS ₂
	cubanite	cb	CuFe ₂ S ₃
	intermediate solid solution	iss	wide range
Fe-Sb-S	berthierite	bt	FeSb ₂ S ₃
	gudmundite	gd	FeSbS
Cu-Fe-Sb-S	tetrahedrite solid solution	td ss	Cu _{12-x} Fe _x Sb ₄ S ₁₃ * 0 ≤ x ≤ 2

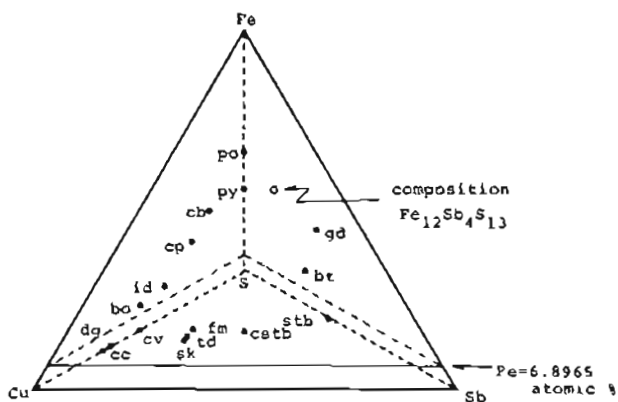


Fig. 1. Natural and synthetic phases in the Cu-Fe-Sb-S system. The name abbreviations used in the present study are given in Table I. The section with Fe = 6.8965 atomic percent corresponds to the stoichiometric composition Cu₁₀Fe₂Sb₄S₁₃.

purity and sulfur powder and antimony crystal grains of 99.999 percent purity were obtained from Nakarai Chemicals Ltd. Prior to use, iron sponge was reduced in a hydrogen stream for at least two hours at 1000°C. Preparation of specimens for the present study is essentially identical to that described by Tatsuka and Morimoto (1973).

In order to investigate the effect of iron on the stability of tetrahedrite solid solution, the shape of the tetrahedrite solid-solution field in the Cu-Fe-Sb-S system was studied by synthesizing specimens with 1.7241, 3.4482, 5.1724, 6.8965, and 7.5172 atomic percent iron. These atomic percents of iron correspond to iron contents of $x = 0.5, 1.0, 1.5, 2.0,$ and $2.18,$ respectively, in the formula of Cu_{12-x}Fe_xSb₄S₁₃. Two-hundred thirty-four specimens were synthesized in the present study.

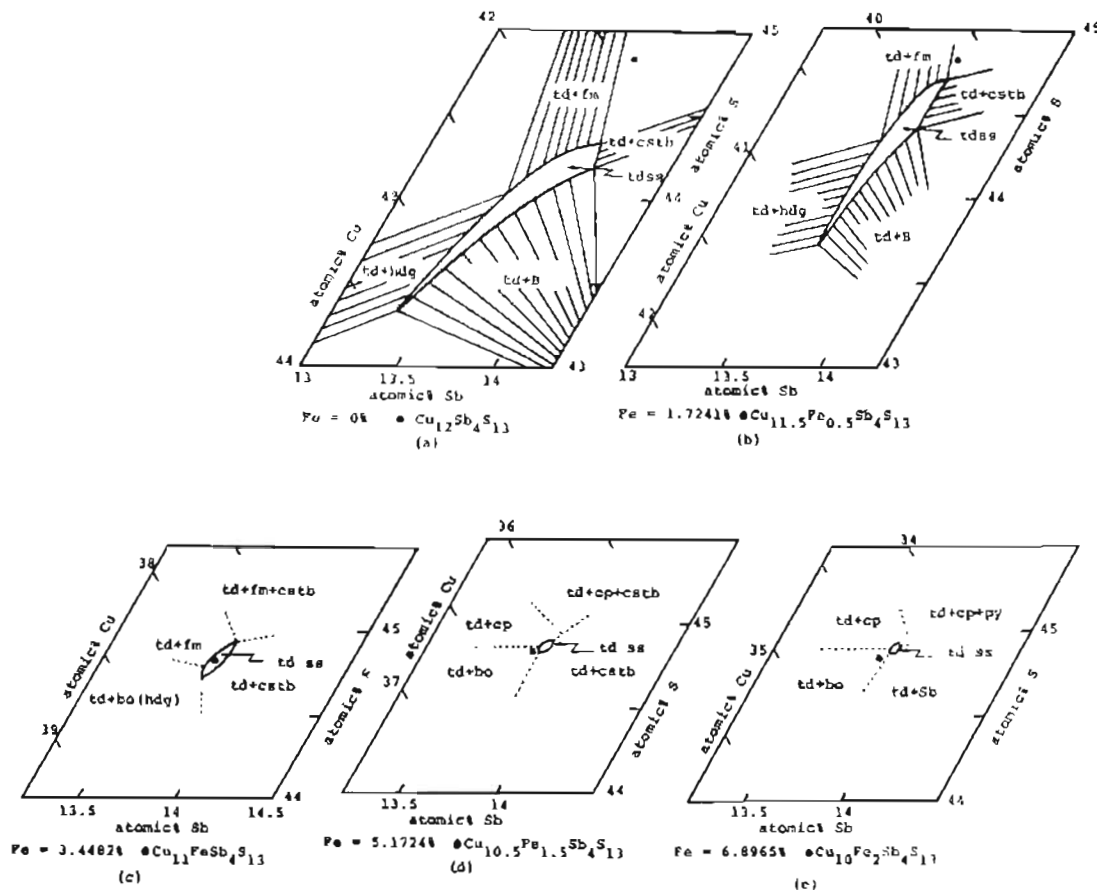


Fig. 2 a-c. Tetrahedrite solid-solution fields at 500°C in the sections with various iron contents of the Cu-Fe-Sb-S composition tetrahedron. Ideal compositions are indicated by solid circles

Reflection microscope and X-ray diffraction methods were employed to identify the phases. The cell dimensions of tetrahedrite were obtained by the X-ray powder method. Density was measured with a pycnometer at 20°C. Fine-powdered specimens (~20 mg) sealed in evacuated silica capsules underwent differential thermal analysis to study the transition, decomposition, and melting behavior of tetrahedrite. A Shimadzu microhardness tester was used for the measurement of Vickers microhardness. Instead of the standard load of 100g, a load of 25g was used because of the small size of crystals. The time of indentation was 15 seconds. Ten indentations were made for each determination, excluding the indentations with excessive fracturing.

Tetrahedrite solid solution in the Cu-Fe-Sb-S system

The tetrahedrite solid-solution field in sections parallel to the Cu-Sb-S face in the Cu-Sb-Fe-S tetrahedron shrinks with increase of iron content at 500°C

(Fig. 2). Therefore tetrahedrite solid solution forms a cone-like shape slightly deviating from the line connecting $\text{Cu}_{12}\text{Sb}_4\text{S}_{13}$ and $\text{Fe}_{12}\text{Sb}_4\text{S}_{13}$ composition, as shown in Figure 3. At 500°C tetrahedrite in the Cu-Sb-S system occupies a narrow solid-solution field at 500°C from $\text{Cu}_{12.28}\text{Sb}_{4.07}\text{S}_{13}$ to $\text{Cu}_{13.02}\text{Sb}_{4.01}\text{S}_{13}$ (Tatsuka and Morimoto, 1973, 1977) (Fig. 2a). In the composition section with 1.7241 atomic percent iron, the tetrahedrite solid-solution field extends from $\text{Cu}_{11.58}\text{Fe}_{0.50}\text{Sb}_{4.07}\text{S}_{13}$ to $\text{Cu}_{12.10}\text{Fe}_{0.51}\text{Sb}_{4.05}\text{S}_{13}$, but does not reach the "ideal" composition $\text{Cu}_{11.5}\text{Fe}_{0.5}\text{Sb}_4\text{S}_{13}$ (Fig. 2b). In the section with 3.4482 atomic percent iron, tetrahedrite solid solution has a small field around the "ideal composition $\text{Cu}_{11}\text{FeSb}_4\text{S}_{13}$ " (Fig. 2c). In the more iron-rich sections with 5.1724 and 6.8965 atomic percent iron, the tetrahedrite solid-solution fields narrow almost to points and are located very near the "ideal" compositions, $\text{Cu}_{10.5}\text{Fe}_{1.5}\text{Sb}_4\text{S}_{13}$ and $\text{Cu}_{10}\text{Fe}_2\text{Sb}_4\text{S}_{13}$ respectively (Figs. 2d and 2e). Single-phase tetrahedrites with the

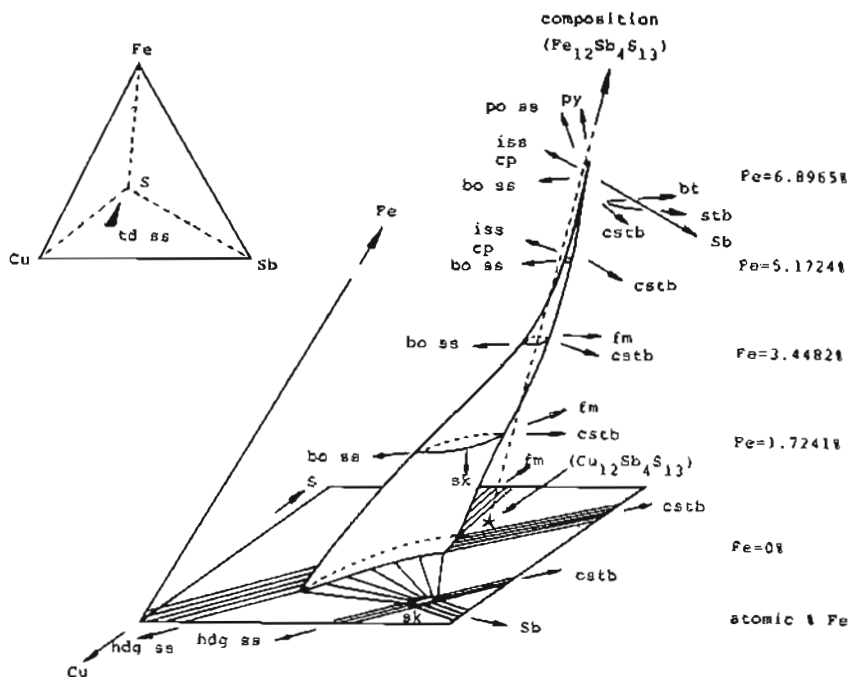


Fig. 3. Sketch of the tetrahedrite solid solution at 500°C in the Cu-Fe-Sb-S composition tetrahedron. All the joins with the tetrahedrite solid solution are shown by the arrows.

"ideal" compositions $\text{Cu}_{10}\text{Fe}_{1.5}\text{Sb}_4\text{S}_{13}$ and $\text{Cu}_{10}\text{Fe}_2\text{Sb}_4\text{S}_{13}$ were not obtained by repeated syntheses, but the compositional differences between the "ideal" compositions and the compositions of the synthetic single-phase tetrahedrites were very slight. In the section with 7.5172 atomic percent iron, thirteen specimens with compositions near the "ideal" composition $\text{Cu}_{9.82}\text{Fe}_{2.18}\text{Sb}_4\text{S}_{13}$ have been synthesized. Tetrahedrite always appeared with chalcopyrite and Sb, and no single-phase tetrahedrite was observed.

Thus, it can be concluded that tetrahedrite in the Cu-Fe-Sb-S system possesses stoichiometric compositions represented by a general ideal formula $\text{Cu}_{12-x}\text{Fe}_x\text{Sb}_4\text{S}_{13}$, where $1 \leq x \leq 2$. This result is consistent with the stoichiometric formula $(\text{Cu,Ag,Fe,Zn})_{12}(\text{Sb,As})_4\text{S}_{13}$ proposed for tetrahedrite (Pauling and Neuman, 1934; Takéuchi, 1971; Springer, 1969).

A sketch of the tetrahedrite solid-solution field in the Cu-Fe-Sb-S system is shown in Figure 3, together with the coexisting phases. The "cone" of the tetrahedrite solid solution extends from a base in the Cu-Sb-S face toward the point $\text{Fe}_{12}\text{Sb}_4\text{S}_{13}$ on the Fe-Sb-S face and terminates at the apex composition $\text{Cu}_{10}\text{Fe}_2\text{Sb}_4\text{S}_{13}$. Tetrahedrite is the only quaternary phase in the Cu-Fe-Sb-S tetrahedron. Selected runs essential to interpretation of the phase relations are presented in Table 2.

This result is consistent with that of Nakamura *et al.* (1974), who reported that tetrahedrite in the Cu-Fe-Sb-S system has a linear solid solution of $(\text{Cu,Fe})_{12}\text{Sb}_4\text{S}_{13}$ with the iron content between 4 and 7.4 weight percent at 475°C based on quantitative microprobe analyses of synthetic specimens.

In order to determine the effect of iron contents on tetrahedrite at low temperatures, tetrahedrite specimens with no iron and with 1.7241 atomic percent iron were annealed at 250°C for two months. The decomposition into famatinitite, digenite, and antimony was observed only in iron-free tetrahedrite, indicating the stability of tetrahedrite with 1.7241 atomic percent iron under this condition. Furthermore, no dissociation of iron-bearing tetrahedrite into two phases was observed in cooling to below 95°C, supporting the effect of a small amount of iron on the stability of tetrahedrite at low temperatures.

Cell dimensions and density in tetrahedrite solid solution

The cell dimensions and density of tetrahedrite of different iron contents along the Cu-poor edge of tetrahedrite solid solution were measured at room temperature. The cell dimensions gradually increase with increase of iron content from 10.3260 Å for an iron-free specimen to 10.3835 Å for a sample contain-

Table 2. Significant experimental runs for the phase relations of tetrahedrite solid solutions in the Cu-Fe-Sb-S system at 500°C. Name abbreviations are given in Table 1

Composition, atomic %				Heating time, Days	Products
Cu	Fe	Sb	S		
39.50	1.7241	13.80	44.9759	35	td+fm+cstb
39.66	1.7241	13.79	44.8259	71	td+fm+cstb
39.90	1.7241	13.70	44.6759	35	td+fm
40.00	1.7241	13.60	44.6759	16	td+fm
40.10	1.7241	13.65	44.5259	35	td+fm
40.15	1.7241	13.55	44.5759	16	td+fm+dg
40.30	1.7241	13.50	44.5759	16	td+fm+dg
40.45	1.7241	13.45	44.3759	16	td+dg
40.55	1.7241	13.55	44.1759	16	td+dg
40.70	1.7241	13.50	44.0759	16	td+dg
39.80	1.7241	13.80	44.6759	71	td
40.10	1.7241	13.70	44.4759	16	td
40.25	1.7241	13.65	44.3759	16	td
40.40	1.7241	13.60	44.2759	16	td
40.50	1.7241	13.70	44.0759	16	td
40.65	1.7241	13.65	43.9759	105	td
40.80	1.7241	13.65	43.8259	105	td
40.95	1.7241	13.50	43.8259	105	td+sk
40.95	1.7241	13.65	43.6759	105	td+sk
40.65	1.7241	13.80	43.8259	35	td+sk
40.45	1.7241	13.85	43.9759	16	td+sk
40.35	1.7241	13.75	44.1759	16	td+sk
40.20	1.7241	13.80	44.4759	16	td+sk
40.30	1.7241	13.90	44.0759	16	td+sk
40.10	1.7241	14.10	44.0759	35	td+sk+cstb
40.00	1.7241	14.00	44.2759	35	td+sk+cstb
39.90	1.7241	13.90	44.6759	71	td+cstb
39.60	1.7241	14.00	44.8259	16	td+cstb
37.75	3.4483	13.80	45.0017	14	td+fm+cstb
37.60	3.4483	13.95	45.0017	14	td+fm+cstb
37.85	3.4483	13.80	44.9071	71	td+fm
37.95	3.4483	13.70	44.9017	71	td+fm
38.10	3.4483	13.70	44.7517	71	td+fm
38.20	3.4483	13.60	44.7517	16	td+dg
38.10	3.4483	13.75	44.7017	105	td+dg
38.10	3.4483	13.80	44.6517	71	td+dg
38.20	3.4483	13.80	44.5517	16	td+dg
37.85	3.4483	13.83	44.8717	35	td
37.93	3.4483	13.79	44.8317	14	td
38.00	3.4483	13.80	44.7517	16	td
38.10	3.4483	13.90	44.6517	16	td+cstb
38.00	3.4483	13.90	44.6517	16	td+cstb
37.90	3.4483	13.90	44.7517	71	td+cstb
38.00	3.4483	13.80	44.7517	35	td+cstb
37.75	3.4483	13.90	44.9017	71	td+cstb
35.95	5.1724	13.85	45.0276	19	td+cp+cstb
35.85	5.1724	13.95	45.0276	19	td+cp+cstb
36.10	5.1724	13.80	44.9276	73	td+cp
36.05	5.1724	13.85	44.9276	19	td+cp
36.15	5.1724	13.80	44.8776	105	td+bo
36.207	5.1724	13.793	44.8276	16	td+bo
36.15	5.1724	13.85	44.8276	19	td+bo+cstb
36.20	5.1724	13.85	44.7776	19	td+bo+cstb
36.10	5.1724	13.85	44.8776	105	td
36.15	5.1724	13.825	44.8526	35	td
36.10	5.1724	13.90	44.8276	20	td+cstb
36.00	5.1724	13.90	44.9286	71	td+cstb
35.90	5.1724	13.95	44.9776	35	td+cstb
34.15	6.8965	13.85	45.1035	19	td+cp+py
34.05	6.8965	13.95	45.1035	19	td+cp+py
34.20	6.8965	13.90	45.0035	35	td+cp
34.25	6.8965	13.90	44.9535	35	td+cp
34.40	6.8965	13.80	44.9035	105	td+cp
34.50	6.8965	13.70	44.9035	105	td+cp
34.40	6.8965	13.70	45.0035	20	td+cp

Table 2. continued.

Composition, atomic %				Heating time, Days	Products
Cu	Fe	Sb	S		
34.48	6.8965	13.79	44.8335	105	td+bo
34.55	6.8965	13.75	44.8035	105	td+bo
34.60	6.8965	13.75	44.7535	105	td+bo
34.35	6.8965	13.85	44.9035	105	td
34.40	6.8965	13.825	44.8785	105	td
34.50	6.8965	13.85	44.7535	105	td+Sb
34.45	6.8965	13.85	44.8035	35	td+Sb
34.30	6.8965	13.90	44.9035	105	td+Sb
33.86	7.5172	13.795	44.8278	35	td+cp+Sb
33.75	7.5172	13.85	44.8828	35	td+cp+Sb
33.65	7.5172	13.90	44.9328	35	td+cp+Sb
33.65	7.5172	13.85	44.9828	24	td+cp+Sb
33.50	7.5172	14.00	44.9828	24	td+cp+Sb
33.45	7.5172	14.05	44.9828	24	td+cp+Sb

ing 6.8965 atomic percent iron (Fig. 4a). However, the density of tetrahedrite decreases from 5.00 for the iron-free specimen to 4.81 for the 6.8965 atomic percent iron specimen (Fig. 4a). The influence of copper-iron replacement on the density variation is relatively small, because the difference in atomic weight between iron and copper is small. It can be concluded that iron atoms simply replace copper atoms in the solid solution and the number of atoms in a unit cell stays constant.

Theoretical density values were calculated from the starting composition by assuming 26 sulfur atoms per unit cell. The measured densities are in good agreement with theoretical values, showing only a systematic difference of about three percent (Fig. 4a).

In the composition plane with 1.7241 atomic percent iron, the tetrahedrite solid-solution field at 500°C expands from near the "ideal" composition ($\text{Cu}_{11.6}\text{Fe}_{0.5}\text{Sb}_4\text{S}_{18}$) to the more copper-rich composition, or more exactly, from $\text{Cu}_{11.58}\text{Fe}_{0.5}\text{Sb}_{4.02}\text{S}_{18}$ to $\text{Cu}_{12.10}\text{Fe}_{0.51}\text{Sb}_{4.05}\text{S}_{18}$. Both cell edge and density increase with increase of copper content from 10.3424 to 10.3789 Å and 4.91 to 5.01, respectively (Fig. 4b). The mass of the unit cell of the copper-rich tetrahedrite is greater by about 3.1 percent than that of the copper-poor end member. This suggests that the composition change of tetrahedrite in a constant iron content section takes place mainly by addition of copper atoms to interstices of the structure. The most copper-rich end member of the solid solution has approximately one more copper atom in each unit cell in comparison with the most copper-poor end member in the section of 1.7241 atomic percent iron. These experimental results are in agreement with

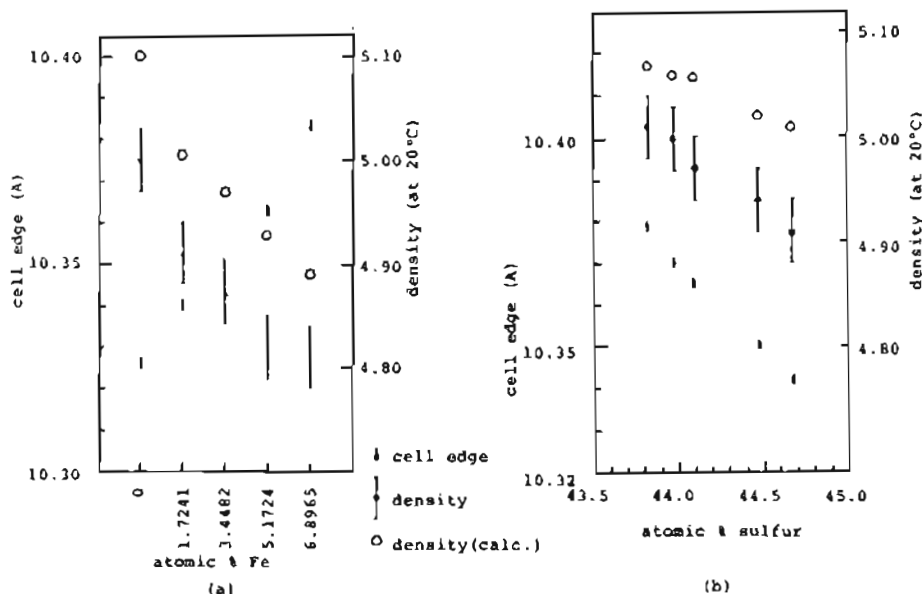


Fig. 4(a) Cell edge and density of the tetrahedrite solid solution plotted against atomic percent of iron. For the specimens with no iron and 1.7241 atomic percent iron, the most copper-poor end members were selected, because they have the nearest compositions to the ideal ones in their solid-solution sections. (b) Cell edge and density of the tetrahedrite solid-solution field with 1.7241 atomic percent iron plotted against atomic percent of sulfur. The calculated values of density (open circles) were obtained by assuming 26 sulfur atoms in a unit cell. Precise values for the cell edge, density, and composition are given in Table 3.

those of Tatsuka and Morimoto (1973). Thus the variation of the cell edge and density of the synthetic tetrahedrite can be explained by two main factors. One is the substitution of copper atoms by other atoms such as iron, zinc, mercury, and silver, and the other is the interstitial addition of copper atoms in a tetrahedrite structure of no or very low iron content.

Wuensch (1964) reports a cell edge of 10.3908 Å for a natural tetrahedrite consisting mainly of copper, iron, zinc, antimony, and sulfur, which is close to 10.3835 Å of synthetic tetrahedrite with the composition $\text{Cu}_{10}\text{Fe}_2\text{Sb}_4\text{S}_{13}$. Half the metal atoms are in tetrahedral coordination sites, and the other half are in three-fold sites. The Cu-S interatomic distances of the mineral are 2.342 Å for the four-coordination copper, and 2.234 and 2.272 Å for the three-coordination copper.

Fe^{2+} atoms occupy preferentially the six- or four-coordination sites in sulfides and sulfoalts in general. The isomer shifts and quadrupole splittings of Mössbauer spectra for synthetic tetrahedrite with a composition of $\text{Cu}_{10.0}\text{Fe}_{2.0}\text{Sb}_4\text{S}_{12.7}$ have shown that iron atoms are tetrahedrally coordinated by four sulfur atoms, and are in the divalent state, Fe^{2+} (Kawai *et al.*, 1972). In tetrahedrite, therefore, the expansion of the cell edge by the substitution of Cu atoms by Fe atoms is considered to be due mainly to the larger ionic radius of Fe^{2+} relative to that of Cu^{2+} .

Some experimental results of interest on copper valency have been obtained by X-ray photoelectron spectroscopy (Nakai *et al.*, 1976). The valence state of copper atoms in some twenty sulfide and sulfoalt minerals, including natural tetrahedrite, are all Cu^{1+} , and no Cu^{2+} has been found. If copper atoms prefer the monovalent state in tetrahedrite of the Cu-Sb-S system, the composition of tetrahedrite in this system must be described as $\text{Cu}_{15}\text{Sb}_4\text{S}_{13}$ by requirement of the electrical charge balance. The existence of the wide solid-solution range of tetrahedrite from $\text{Cu}_{12.11}\text{Sb}_{4.09}\text{S}_{13}$ to $\text{Cu}_{13.77}\text{Sb}_{4.08}\text{S}_{13}$ (Tatsuka and Morimoto, 1973) in the Cu-Sb-S system at 300°C suggests that copper atoms exist in two ionic states, Cu^{1+} and Cu^{2+} , with preference of Cu^{1+} over Cu^{2+} .

Melting temperature and Vickers microhardness

Both melting temperature and Vickers microhardness vary systematically with the iron content of tetrahedrite solid solution. The Vickers microhardness varies from 300 to 380 kg/mm² with increasing iron content, in spite of a decrease in density (Fig. 5a). The Vickers microhardness reported by Hall (1972) is consistent with the present results.

In order to examine the change in the melting temperatures of iron-bearing tetrahedrite, differential thermal analyses of tetrahedrite solid solution along

the Cu-poor edge were carried out (Fig. 6). The melting temperature apparently rises from 573° to 661°C with increase in iron content (Fig. 5b). However, microscopic observations of the quenched products indicated that tetrahedrite with less than 1.7241 atomic percent iron decomposes below the melting temperature, whereas tetrahedrite with more than 3.4482 atomic percent iron does not decompose prior to melting.

Because the specimen used for the DTA measurement in this investigation was the copper-poor tetrahedrite $\text{Cu}_{12.30}\text{Sb}_{4.05}\text{S}_{13}$ (Table 3a), it first breaks down to famatinite + chalcocite + high-skinnerite at about 543°C. Two endothermic peaks starting at 573°C and 584°C are considered to indicate the melting of the decomposition products.

The copper-poor tetrahedrite $\text{Cu}_{11.58}\text{Fe}_{0.5}\text{Sb}_{4.02}\text{S}_{13}$ (1.7241 atomic percent iron) (Table 3a) breaks down to famatinite + chalcocite + tetrahedrite at about 570°C. The endothermic peak beginning at 594°C may correspond to melting of the decomposition products. The tetrahedrite $\text{Cu}_{10.46}\text{Fe}_{1.50}\text{Sb}_{4.01}\text{S}_{13}$ does not break down at temperatures below the melting point. The endothermic peak beginning at 643°C corresponds to the incongruent melting to liquid and a more iron-rich tetrahedrite phase. The final tetrahedrite in this incongruent melting is $\text{Cu}_{0.96}\text{Fe}_2\text{Sb}_4\text{S}_{13}$, which melts at 661°C. For the tetrahedrite $\text{Cu}_{11}\text{FeSb}_4\text{S}_{13}$, the endothermic peak shows some intermediate shape between $\text{Cu}_{11.58}\text{Fe}_{0.5}\text{Sb}_{4.02}\text{S}_{13}$ and $\text{Cu}_{10.46}\text{Fe}_{1.50}\text{Sb}_{4.01}\text{S}_{13}$. However, microscopic observa-

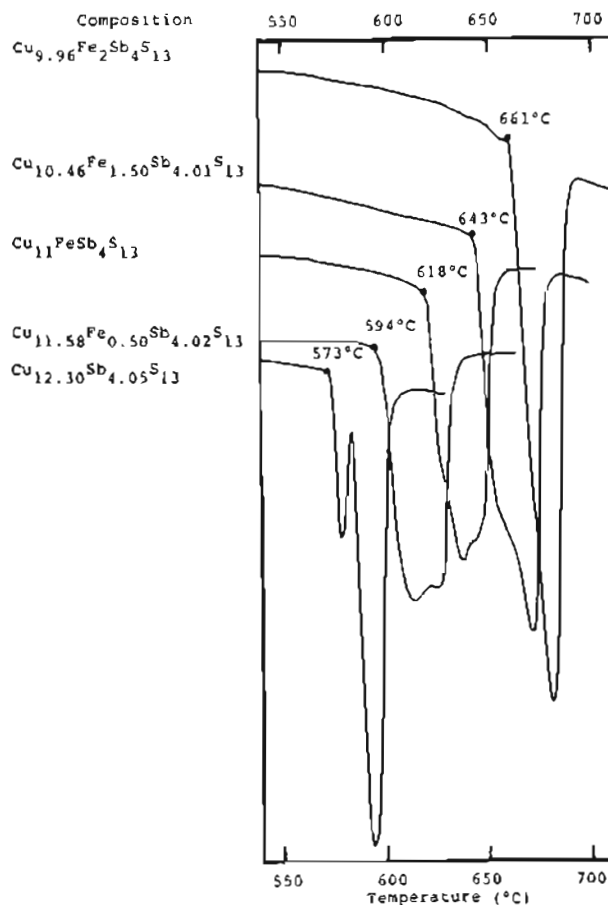


Fig. 6 DTA curves of synthetic tetrahedrite in the Cu-Fe-Sb-S system. Compositions of the specimens are given in Table 3a

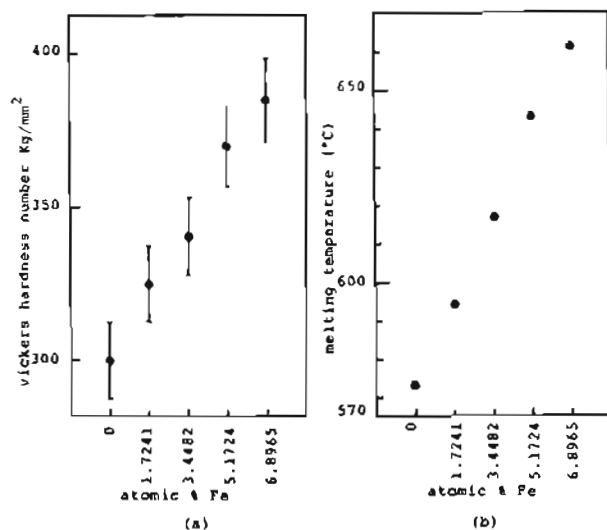


Fig. 5 Vickers microhardness and melting temperature in the tetrahedrite solid solution. Composition of the specimens are given in Table 3a.

tion of the quenched products indicated that the melting of $\text{Cu}_{11}\text{FeSb}_4\text{S}_{13}$ is of the same type as that of $\text{Cu}_{10.46}\text{Fe}_{1.50}\text{Sb}_{4.01}\text{S}_{13}$.

The almost symmetrical endothermic peak starting at 661°C shows congruent melting of tetrahedrite $\text{Cu}_{0.96}\text{Fe}_2\text{Sb}_4\text{S}_{13}$, which is very near the stoichiometric composition. These results indicate that the thermal stability range of tetrahedrite gradually increases with increasing iron content. However, the role of iron atoms for the stabilization of tetrahedrite is not clear at this stage.

Stability and assemblages of tetrahedrite

Tetrahedrite solid solution can coexist at 500°C with almost all stable phases in the Cu-Sb-S, Cu-Fe-S, and Fe-Sb-S systems. Only covellite does not form a join with tetrahedrite solid solution. Digenite-bornite solid solution coexists with tetrahedrite solid solution over the entire compositional range. Chalcocite coexists with tetrahedrite solid solution

Table 3. Cell edges, densities, and compositions of tetrahedrite solid solutions.

	composition								cell edge	density	
	atomic percent				chemical formula (S=13)				a (Å)	at 25°C	
	Cu	Fe	Sb	S	Cu	Fe	Sb	S	±0.002	±0.03	calc.
(a)	41.90	0	13.80	44.30	12.30	0	4.05	13	10.3260	5.00	5.099
	39.80	1.7241	13.80	44.6759	11.58	0.50	4.02	13	10.3424	4.91	5.011
	37.93	3.4483	13.79	44.8317	11.00	1.00	4.00	13	10.3499	4.87	4.967
	36.10	5.1724	13.85	44.8776	10.46	1.50	4.01	13	10.3661	4.82	4.928
	34.40	6.8965	13.825	44.8785	9.96	2.00	4.00	13	10.3835	4.81	4.891
(b)	39.80	1.7241	13.80	44.6759	11.58	0.50	4.02	13	10.3424	4.91	5.011
	40.10	1.7241	13.70	44.4759	11.72	0.50	4.00	13	10.3508	4.94	5.022
	40.50	1.7241	13.70	44.0759	11.95	0.51	4.04	13	10.3649	4.97	5.058
	40.65	1.7241	13.65	43.9759	12.02	0.51	4.04	13	10.3705	5.00	5.061
	40.80	1.7241	13.65	43.8259	12.10	0.51	4.05	13	10.3789	5.01	5.070

containing up to about five atomic percent iron. Famatinite and high-temperature skinnerite form joins with tetrahedrite solid solution with up to about 3.5 and 1.7 atomic percent iron, respectively. Tetrahedrite solid solution with more than about five atomic percent iron can coexist with chalcopyrite solid solution, intermediate solid solution, pyrrhotite solid solution, pyrite, stibnite, berthierite, and antimony.

Natural tetrahedrite shows complex compositions in which As and Sb display extensive mutual substitution, and elements such as Fe, Zn, Hg, and Ag commonly substitute for Cu. Phase relations in the system Cu-Sb-As-S were studied by Luce *et al.* (1977). It has been shown that silver atoms preferentially occupy three-coordinated positions (Kalbskopf, 1972) and that mercury atoms substitute only for copper atoms tetrahedrally coordinated with sulfur (Kalbskopf, 1971).

Chemical compositions of natural tetrahedrite strongly support the conclusion that the minerals belonging to the tetrahedrite-tennantite series have a general formula, $(\text{Cu,Ag})_{10}(\text{Fe,Zn,Hg,Cu}^*)_2(\text{Sb,As})_2\text{S}_{13}$ (Pauling and Neuman, 1934; Takéuchi, 1971; Springer, 1969). According to Charlat and Levy (1974), Cu* in the (Fe,Zn,Hg) sites is limited less than 0.2 atom in most natural specimens. Only when more than one atom Fe is in the (Fe,Zn,Hg) sites can as much as 0.8 atom Cu* be included in the same sites in some cases, suggesting that more Cu-rich tetrahedrites than $\text{Cu}_{10.8}\text{Fe}_{1.2}\text{Sb}_4\text{S}_{13}$ are not stable. Thus, although tetrahedrite $\text{Cu}_{11.8}\text{Fe}_{0.5}\text{Sb}_4\text{S}_{13}$ was apparently stable at room temperature in the present experiments, it is most likely that such tetrahedrite decom-

poses in nature to the mixture of more iron-rich tetrahedrite $\text{Cu}_{10-10.8}\text{Fe}_{2-1.2}\text{Sb}_4\text{S}_{13}$, famatinite, digenite, and antimony.

Acknowledgments

We thank Professor T. Nakamura, Osaka City University, for the use of the microhardness tester. We also thank Professor B. J. Skinner, Yale University, for sharing the manuscript of a paper on the Cu-Sb-As-S system before publication and comments made during review, and Professor G. Kullerud, Purdue University, for his discussion and comments on the results of this work. Suggestions made, during review, by Professor Ulrich Petersen, Mr. Robert R. Loucks, and Mr. John C. Tanger are appreciated. Part of the expenses of this work were defrayed by a grant for scientific research from the Ministry of Education of the Japanese Government.

References

- Charlat, M. and C. Levy (1974) Substitutions multiples dans la série tennantite-tétraédrite. *Bull. Soc. fr. Minéral. Cristallogr.*, 97, 241-250.
- Hall, A. J. (1972) Substitution of Cu by Zn, Fe and Ag in synthetic tetrahedrite, $\text{Cu}_{12}\text{Sb}_4\text{S}_{13}$. *Bull. Soc. fr. Minéral. Cristallogr.*, 95, 583-594.
- (1974) The effect of substitution of Cu by Zn, Fe and Ag on the optical properties of synthetic tetrahedrite, $\text{Cu}_{12}\text{Sb}_4\text{S}_{13}$. *Bull. Soc. fr. Minéral. Cristallogr.*, 97, 18-26.
- Kalbskopf, R. (1971) Die Koordination des Quecksilbers im Schwazit. *Tschermaks Mineral. Petrog. Mitt.*, 16, 173-175.
- (1972) Strukturverfeinerung des Freibergits *Tschermaks Mineral. Petrog. Mitt.*, 18, 147-155.
- Kawai, S., Y. Ito, and R. Kiriyama (1972) Magnetic susceptibility, Mössbauer effect and conductivity in sphalerite and tetrahedrite (in Japanese). *J. Mineral. Soc. Japan*, 10, 487-498.
- Luce, F. D., C. L. Tuttle and B. J. Skinner (1977) Studies of sulfosalts of copper. V. Phases and phase relations in the system Cu-Sb-As-S between 350°C and 500°C. *Econ. Geol.*, 72, 271-289.
- Nakai, I., Y. Sugitani, Y. Niwa and K. Nagashima (1976) Application of X-ray photoelectron spectra for copper ore minerals

- (abstr. in Japanese) *Abstr. Annual Meet. Mineral. Soc. Japan*, 101, B41.
- Nakamura, Y., A. Sugaki, H. Shima, and A. Kitakaze (1974) The phase relations in the Cu-Fe-Sb-S system (II) Tetrahedrite-bornite solid solution (abstr. in Japanese). *J. Jap. Assoc. Mineral. Petrol. Econ. Geol.*, 69, 42.
- Pauling, L., and E. W. Neuman (1934) The crystal structure of binnite, $(\text{Cu,Fe})_{12}\text{As}_4\text{S}_{13}$ and the chemical composition and structure of minerals of the tetrahedrite group. *Z. Kristallogr.*, 88, 54-62.
- Skinner, B. J., F. D. Luce and E. Makovicky (1972) Studies of the sulfosalts of copper. III. Phases and phase relations in the system Cu-Sb-S. *Econ. Geol.*, 67, 924-938.
- Springer, G. (1969) Electronprobe analyses of tetrahedrite. *Neus Jahrb. Mineral. Monatsh.*, 24-32.
- Sugaki, A., J. Shima and A. Kitakaze (1972) The differential thermal analysis of ore minerals (III). On the minerals of system Bi-Sb-S and Cu-Sb-As-S (in Japanese) *Mem. Fac. Eng. Yamaguchi Univ.*, 23, 23-33.
- Takéuchi, Y. (1971) On the crystal chemistry of sulphides and sulphosalts. In T. Tatsumi, Ed., *Volcanism and Genesis in Japan*, p. 395-420 Univ. of Tokyo Press, Tokyo.
- Tatsuka, K., and N. Morimoto (1973) Composition variation and polymorphism of tetrahedrite in the Cu-Sb-S system below 400°C. *Am. Mineral.*, 58, 425-434.
- and —— (1977) Tetrahedrite stability relations in the Cu-Sb-S system. *Econ. Geol.*, 72, 258-270.
- Wuensch, B. J. (1964) The crystal structure of tetrahedrite, $\text{Cu}_{12}\text{Sb}_4\text{S}_{13}$. *Z. Kristallogr.*, 119, 437-453.

Manuscript received, February 14, 1977; accepted for publication, June 13, 1977.